

MENEZES, I., CAPELO-NETO, J., PESTANA, C.J., CLEMENTE, A., HUI, J., IRVINE, J.T.S., GUNARATNE, H.Q.N., ROBERTSON, P.K.J., EDWARDS, C., GILLANDERS, R.N., TURNBULL, G.A. and LAWTON, L.A. 2021. Comparison of UV-A photolytic and UV/TiO₂ photocatalytic effects on *Microcystis aeruginosa* PCC7813 and four microcystin analogues: a pilot scale study. *Journal of environmental management* [online], 298, article 113519. Available from: <https://doi.org/10.1016/j.jenvman.2021.113519>

Comparison of UV-A photolytic and UV/TiO₂ photocatalytic effects on *Microcystis aeruginosa* PCC7813 and four microcystin analogues: a pilot scale study.

MENEZES, I., CAPELO-NETO, J., PESTANA, C.J., CLEMENTE, A., HUI, J., IRVINE, J.T.S., GUNARATNE, H.Q.N., ROBERTSON, P.K.J., EDWARDS, C., GILLANDERS, R.N., TURNBULL, G.A. and LAWTON, L.A.

2021

1 **Comparison of UV-A photolytic and UV/TiO₂ photocatalytic effects on**
2 ***Microcystis aeruginosa* PCC7813 and four microcystin analogues: a pilot**
3 **scale study**

4

5 Indira Menezes^{a,b*}, José Capelo-Neto^a, Carlos J. Pestana^b, Allan Clemente^a, Jianing
6 Hui^c, John T. S. Irvine^c, H.Q. Nimal Gunaratne^d, Peter K.J. Robertson^d, Christine
7 Edwards^b, Ross N. Gillanders^e, Graham A. Turnbull^e, Linda A. Lawton^b

8

9 ^a Department of Hydraulic and Environmental Engineering, Federal University of Ceará,
10 Fortaleza, Brazil

11 ^b School of Pharmacy and Life Sciences, Robert Gordon University, Aberdeen, United
12 Kingdom

13 ^c School of Chemistry, University of St Andrews, St Andrews, United Kingdom

14 ^d School of Chemistry and Chemical Engineering, Queen's University, Belfast, United
15 Kingdom

16 ^e Organic Semiconductor Centre, SUPA, School of Physics and Astronomy, University
17 of St Andrews, St Andrews, United Kingdom

18

19 *Corresponding author: i.de-menezes-castro@rgu.ac.uk

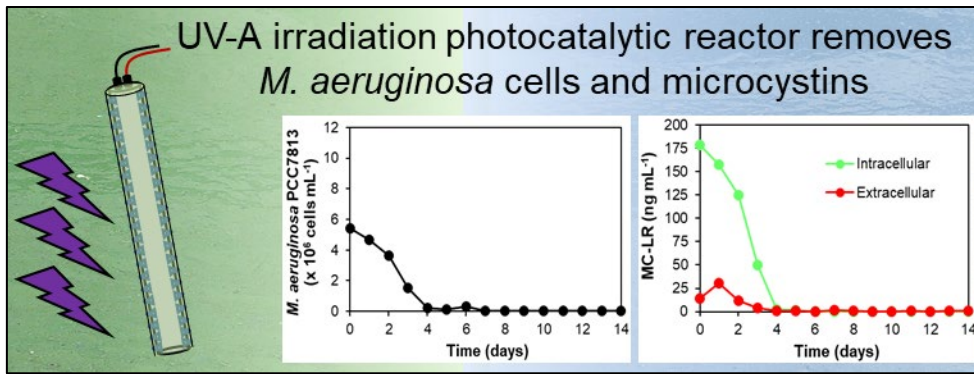
20

21 **Highlights**

- 22 • UV-A photolysis was effective for elimination of cyanobacteria and toxins
- 23 • Complete inhibition of *M. aeruginosa* PCC7813 by UV-A photolysis
- 24 • 92% removal of four microcystins after UV-A photolysis (intra- and extracellular)
- 25 • TiO₂ photocatalysis was less effective in *M. aeruginosa* PCC7813 cell removal

26

27 **Graphical abstract**



28

29

30 **Abstract**

31 To date, the high cost of supplying UV irradiation has prevented the widespread
 32 application of UV photolysis and titanium dioxide based photocatalysis in removing
 33 undesirable organics in the water treatment sector. To overcome this problem, the use
 34 of UV-LEDs (365 nm) for photolysis and heterogeneous photocatalysis applying TiO₂
 35 coated glass beads under UV-LED illumination (365 nm) in a pilot scale reactor for the
 36 elimination of *Microcystis aeruginosa* PCC7813 and four microcystin analogues (MC-
 37 LR, -LY, -LW, -LF) with a view to deployment in drinking water reservoirs was
 38 investigated. UV-A (365 nm) photolysis was shown to be more effective than the
 39 UV/TiO₂ photocatalytic system for the removal of *Microcystis aeruginosa* cells and
 40 microcystins. During photolysis, cell density significantly decreased over 5 days from
 41 an initial concentration of 5.8 x 10⁶ cells mL⁻¹ until few cells were left. Both intra- and
 42 extracellular microcystin concentrations were significantly reduced by 100 and 92%,
 43 respectively, by day 5 of the UV treatment for all microcystin analogues. During
 44 UV/TiO₂ treatment, there was great variability between replicates, making prediction of
 45 the effect on cyanobacterial cell and toxin behavior difficult.

46

47 **Keywords:** blue-green algae; cyanotoxins; water treatment; titanium dioxide,
 48 cyanobacteria

49 **1 Introduction**

50 Cyanobacterial blooms in freshwater reservoirs represent a threat to human and animal
51 health because of the potential release of a wide variety of harmful metabolites, known
52 collectively as cyanotoxins (Carmichael *et al.*, 2001; Falconer *et al.*, 1983; Jochimsen
53 *et al.*, 1998). Microcystins (MCs) are one of the most commonly reported cyanotoxins
54 with over 247 analogues to date (Spoof and Catherine, 2017). Conventional water
55 treatment (i.e., coagulation, flocculation, sedimentation or flotation and filtration) is used
56 worldwide for treatment of water contaminated with cyanobacteria, however, these
57 processes can promote cell rupture and consequently cyanotoxin release into the
58 environment (Chang *et al.*, 2018; Pestana *et al.*, 2019). Further, conventional treatment
59 methods are designed for the removal of suspended or colloidal particles and are not fit
60 to remove dissolved contaminants including dissolved cyanotoxins (Chae *et al.*, 2019;
61 Vilela *et al.*, 2012). In order to mitigate the effect of dissolved cyanobacterial toxins
62 entering water treatment plants, advanced oxidation processes (AOPs) such as
63 photocatalysis and photolysis can be used for the control of cyanobacterial cells and
64 toxic metabolites within reservoirs (Fan *et al.*, 2019; Matthijs *et al.*, 2012; Ou *et al.*,
65 2011a).

66 UV photolysis is an AOP that has been widely applied for the inactivation of pathogenic
67 microbes in water treatment and other applications, and can be used as a strategy for
68 removing cyanobacteria and their toxins. A number of studies have evaluated the
69 effects of mainly UV-C (usually 254 nm) and UV-B (usually 312 nm) on microcystin
70 degradation and *Microcystis aeruginosa* removal (Liu *et al.*, 2010; Moon *et al.*, 2017;
71 Tao *et al.*, 2018). This, however, is the first time that the degradation of *M. aeruginosa*
72 PCC7813 and four microcystin analogues (MC-LR, MC-LW, MC-LY, MC-LF) under UV-
73 A (365 nm) irradiation was investigated.

74 UV-irradiation-driven titanium dioxide (TiO₂) photocatalysis is another AOP that can be
75 used to control cyanobacteria and their toxins. TiO₂ activation needs to occur under UV
76 light irradiation ($\lambda < 387$ nm) (Chang *et al.*, 2018; Hu *et al.*, 2017; Zhao *et al.*, 2014) due
77 to its wide band gap (3.2 eV and 3.0 eV for the anatase and rutile forms of TiO₂

78 respectively) (Chen *et al.*, 2015; Hu *et al.*, 2017; Pinho *et al.*, 2015b), which limits its
79 application in drinking water treatment (Jin *et al.*, 2019). UV light is, however,
80 attenuated by water and hence the need for UV irradiation (below 387 nm) is a hurdle
81 in the practical application of photolysis and photocatalysis for water treatment (Chae
82 *et al.*, 2019). To overcome this, and to make the systems practical for application in
83 reservoirs used for drinking water, the system investigated here employs UV (365 nm)
84 light emitting diodes (LEDs), which are low-cost (ca. USD 0.78 per LED), long life
85 (approximately 100,000 working hours; Heering, 2004) and capable of activating TiO₂.
86 In the current study, UV-LED-driven photolysis and TiO₂ photocatalysis were evaluated
87 over 14 days for the elimination of *M. aeruginosa* PCC7813 as well as for the
88 destruction of four microcystin analogues (MC-LR, MC-LW, MC-LY, MC-LF).

89

90 **2 Methods**

91 **2.1 Reagents**

92 The chemicals for artificial fresh water (AFW) and BG-11 culture medium (Stanier *et al.*,
93 1971) preparation were of reagent grade (Fisher Scientific, UK). AFW was prepared
94 according to Akkanen and Kukkonen (2003) by dissolving CaCl₂ (11.8 mg L⁻¹), MgSO₄
95 (4.9 mg L⁻¹), NaHCO₃ (2.6 mg L⁻¹) and KCl (0.2 mg L⁻¹) in ultrapure water. For AFW,
96 pH was adjusted to 7 with 1 M hydrochloric acid or 1 M sodium hydroxide if required.
97 Acetonitrile, methanol, and trifluoroacetic acid used for high performance liquid
98 chromatography analysis of microcystins were of HPLC grade (Fisher Scientific, UK).
99 Diuron (3-(3,4-dichlorophenyl)-1,1-dimethylurea) (Sigma-Aldrich, UK) was used for
100 photosynthetic activity assays. Isoton II Diluent obtained from Beckman Coulter (USA)
101 was used for cyanobacterial cell density determination. All solutions were prepared
102 using ultrapure water (18.2 MΩ) provided by an ELGA PURELAB system (Veolia, UK).

103

104 **2.2 Cyanobacterial cultivation**

105 The cyanobacterium *M. aeruginosa* PCC7813 (Pasteur Culture Collection) was grown

106 in BG-11 medium at 21 ± 1 °C with constant cool white fluorescent illumination with an
107 average light intensity of $30 \mu\text{mol photons m}^{-2} \text{s}^{-1}$ and constant sparging with sterile air.
108 This strain does not have gas vesicles and produces four main microcystin analogues
109 (MC-LR, MC-LY, MC-LW and MC-LF).

110

111 **2.3 Reactor design for *M. aeruginosa* PCC7813 and microcystins treatment**

112 A cell suspension of a 27 days-old culture of *M. aeruginosa* PCC7813 (5×10^6 cells mL⁻¹)
113 in AFW was prepared and sampled prior to addition to the reactors (C_0). The reactors
114 (1000 x 90 mm) were made of a stainless-steel mesh with an aperture of 1.2 x 1.2 mm
115 and 0.4 mm wire strength. Each reactor was placed inside an acrylic cylinder (1100 x
116 95 mm) that was filled with 6.5 liters of *M. aeruginosa* suspension. The acrylic cylinders
117 were sparged from the bases through a multi-porous air-stone with sterile air with the
118 aid of a pump for continuous gentle air flow (1 L min^{-1} per reactor; Figure S1). The top
119 of the acrylic cylinders was covered with a foam bung to avoid external contamination
120 and to allow air exchanges. The overhead ambient light was of low intensity ($2.5 \mu\text{mol}$
121 $\text{photons m}^{-2} \text{s}^{-1}$). Triplicate reactors were prepared for each of the tested systems (UV-
122 only, TiO₂-only and UV/TiO₂).

123 One set of three reactors for the UV-A treatment (photolysis) was prepared (Figure
124 S1A) which consisted of reactors with 5 UV-LED strips (1 meter), each with 120
125 individual UV-LEDs ($\lambda=365 \text{ nm}$ and light intensity of 5 W m^{-2}), attached to the external
126 surface of the acrylic cylinders and 6.5 L of the cyanobacterial cell suspension added.
127 In the UV-A treatment, empty tetrahedral stainless-steel wire mesh pods (aperture 1.2 x
128 1.2 mm, wire strength 0.4 mm, Figure S2) were placed inside the reactors without TiO₂
129 coated glass beads to allow observation of the effects of only UV-A light on *M.*
130 *aeruginosa* PCC7813 and its four microcystin analogues. To determine if the TiO₂
131 coated beads have an effect on the cyanobacterial cells and toxins in the absence of
132 UV light, a second set of triplicate reactors was prepared (Figure S1B), consisting of
133 6.5 L of the *M. aeruginosa* PCC7813 suspension and TiO₂ coated glass beads (3.2 g)

134 corresponding to 0.1% (w/v) TiO₂ inside tetrahedral stainless-steel pods (Figure S2).
135 The TiO₂ coated beads were manufactured from recycled glass that were prepared as
136 per Pestana *et al.* (2020) and Hui *et al.* (2021) containing approximately 12% (w/w)
137 TiO₂. In the TiO₂-only samples, no UV illumination was used. Finally, a third set of
138 reactors to test the efficacy of TiO₂ photocatalysis was prepared. The UV/TiO₂
139 treatment consisted of reactors with TiO₂ coated glass beads inside of the stainless-
140 steel pods (Figure S2), 5 UV-LED strips and 6.5 liters of *M. aeruginosa* cell suspension
141 (Figure S1C). All reactors were maintained in the presence low light intensity (2.5 μmol
142 photons m⁻² s⁻¹) from overhead lighting since photosynthetic organisms like
143 cyanobacteria require light to survive.

144 Samples were collected and temperature measured (supplementary material S2) at the
145 same time every day over 14 days. A total of 4 mL was removed at each sampling
146 point, of which 1.5 mL was used for cell enumeration, 1.5 mL was used for
147 intra/extracellular microcystin analysis and 1 mL was used for photosynthetic activity
148 measurements. All aliquots were used immediately except for the aliquots for toxin
149 determination, which were centrifuged for 10 minutes at 13000 G and the supernatant
150 and cell pellets were stored separately at -20 °C until further processing and analysis.

151

152 **2.4 *M. aeruginosa* PCC7813 regrowth experiment**

153 To assess the regrowth of *M. aeruginosa* PCC7813 after 14 days treatment, samples
154 (50 mL) were removed from each reactor and mixed with an equal volume of BG-11
155 medium. Aliquots of this mixture (3 mL) were transferred to 28 sterile glass vials (4 mL
156 volume) to allow for sacrificial sampling over seven days with four replicate samples.
157 Samples for each sampling point (i.e., 4 vials) were incubated in a sterile glass beaker
158 (150 mL), covered with a sterile petri dish lid (Figure S3). Immediately, one set of
159 samples was removed and cell density was analyzed (C₀ sample), the remaining
160 beakers were incubated at 21±1 °C on a 12/12 hours light/dark cycle illuminated by
161 cool white fluorescent lights with an average light intensity of 10.5 μmol photons m⁻² s⁻¹

162 without agitation for the following 6 days and sampled at the same time every day.

163

164 **2.5 Analysis**

165 **2.5.1 *M. aeruginosa* PCC7813 cell density determination**

166 *M. aeruginosa* PCC7813 cell density was measured with a Multisizer 3 (Beckman
167 Coulter, USA). A 50 µm aperture tube was used to detect particle sizes from 1 to 7 µm
168 for both reactor treatments and regrowth experiments. Samples were diluted 200 to
169 1500-fold in Isoton II Diluent (Beckman Coulter, USA), depending on the sample cell
170 density.

171

172 **2.5.2 *M. aeruginosa* PCC7813 photosynthetic activity evaluation**

173 A Mini-PAM system (Walz, Germany) was used for cyanobacterial photosynthetic
174 activity analysis according to Menezes *et al.* (2020). In short, the minimal fluorescence
175 F_0 was measured by adding 400 µL of sample into a cuvette under agitation followed
176 by diuron (0.5 M) addition (20 µL) and the true maximal fluorescence measurement
177 (F_M') by a saturating pulse under actinic light. The cyanobacterial photosynthetic activity
178 can be determined by the maximal values of quantum yield of photosystem (PS) II
179 calculated by F_V/F_M' , where F_V is the difference between F_M' and F_0 (Stirbet *et al.*,
180 2018).

181

182 **2.5.3 Intra- and extracellular microcystin determination by high-performance** 183 **liquid chromatography (HPLC)**

184 After sampling, the liquid and solid portions of the sample were separated in a
185 centrifuge for 10 minutes at 13000 G. The supernatant, representing the extracellular
186 toxin component, was evaporated to dryness in an EZ-II evaporator (Genevac, UK).
187 Dried samples were resuspended in 80% aqueous methanol (150 µL) and stored at -
188 20 °C until analysis. Cell pellets, representing the intracellular toxin component, were
189 resuspended in 80% aqueous methanol (150 µL), agitated in a dispersive extractor for

190 5 minutes at 2500 rpm and centrifuged for 10 minutes at 13000 G to remove cell
 191 debris. The resultant supernatant, representing the liberated intracellular content was
 192 stored at -20 °C until analysis. The concentrations of four microcystin analogues (MC-
 193 LR, MC-LY, MC-LW and MC-LF) were quantified by HPLC (Table 1).

194

195 **Table 1** – Analytical conditions of HPLC for intra- and extracellular microcystins
 196 determination.

Parameters	Conditions
HPLC	2965 separation module and a 2996 photodiode array (PDA) detector (Waters, United States)
Column	Symmetry C18 column, 2.1 mm x 150 mm, 5 µm particle size (Waters, United States)
Mobile phase	A: 0.05% trifluoroacetic acid in ultrapure water (18.2 MΩ) B: 0.05% trifluoroacetic acid in acetonitrile
Gradient	Time (min) 0 25 26 29 35 Solvent A (%) 80 30 0 80 80
Flow rate	0.3 mL min ⁻¹
Injection volume	35 µL
Column temperature	40 °C
PDA scan range	200-400 nm

197

198 All chromatograms were extracted at 238 nm and quantified using standards (as per
 199 Enzo Life Sciences) for calibration between 0.001 and 5 µg mL⁻¹ in the Empower
 200 software. The limit of quantification was 0.01 µg mL⁻¹ for MC-LF and 0.005 µg mL⁻¹ for
 201 the other microcystin analogues.

202

203 **2.7 Statistical data analyses**

204 All statistical analyses were performed using RStudio with a significance level of 5%. In
 205 order to verify if the TiO₂-only samples, UV and UV/TiO₂ treatments influenced cell
 206 numbers or toxin removal it is necessary to identify a significant reduction of cell
 207 density during treatment and intra- and extracellular microcystin concentration
 208 (dependent variables) over 14 days (independent variable). The results were pre-
 209 analyzed using different statistical models, i.e., linear, piecewise, linear-plato,

210 exponential and logarithmic regression. The models were selected and adjusted using
211 the linear or piecewise regression techniques using the mean of triplicates from each
212 treatment group. The linear or piecewise regression techniques were selected because
213 they were the models that presented the best fit with the data. The mean was selected
214 to create each model because the mean values presented normal distribution
215 according to Shapiro-Wilk Normality Test (data not shown). The linear regression
216 consists in a linear relation between dependent (cell density and microcystins
217 concentration) and independent (time) variables. The piecewise regression consists in
218 multiple linear models to the data for different ranges of the independent variable,
219 which means that the tendency/inclination of the curve of the dependent variable will
220 change over the independent variable. A detailed description of the data analysis and
221 the model selection can be found in the supplementary material (S4).

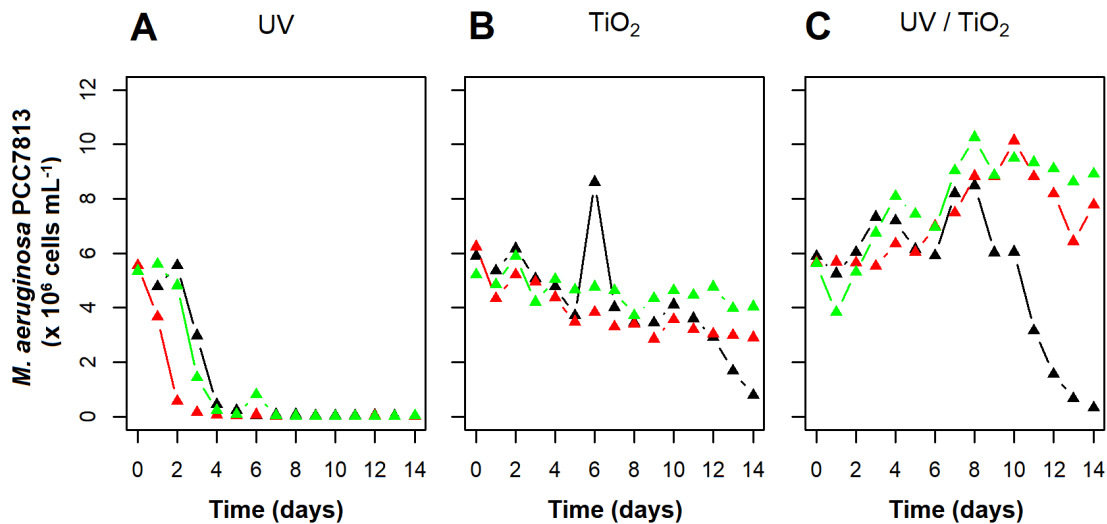
222

223 **3 Results and Discussion**

224 **3.1 Treatment effects on *Microcystis aeruginosa* PCC7813 cell density and** 225 **photosynthetic activity**

226 The removal of *M. aeruginosa* PCC7813 in a photocatalytic and a photolytic reactor
227 using UV-LEDs and TiO₂ coated beads was investigated. The effect of the UV-A
228 treatment presented a piecewise regression tendency (Figure S4) with a cell density
229 decrease from 5.4×10^6 cells mL⁻¹ over 5 days until there were only 1.8×10^4 cells mL⁻¹
230 left (significant tendency rate of 1.12×10^6 cells mL⁻¹ day⁻¹ until 5 days, $p < 0.01$; Figure
231 1A).

232



233

Figure 1 – Effects of (A) UV-LED irradiation (365 nm), (B) TiO_2 coated glass beads under ambient light ($2.5 \mu\text{mol photons m}^{-2} \text{s}^{-1}$) and (C) photocatalytic treatment on *Microcystis aeruginosa* PCC7813 cell density using TiO_2 coated glass beads under UV-LED illumination (365 nm) over 14 days, sparged with sterile air. Data points represent individual replicates for each treatment.

234

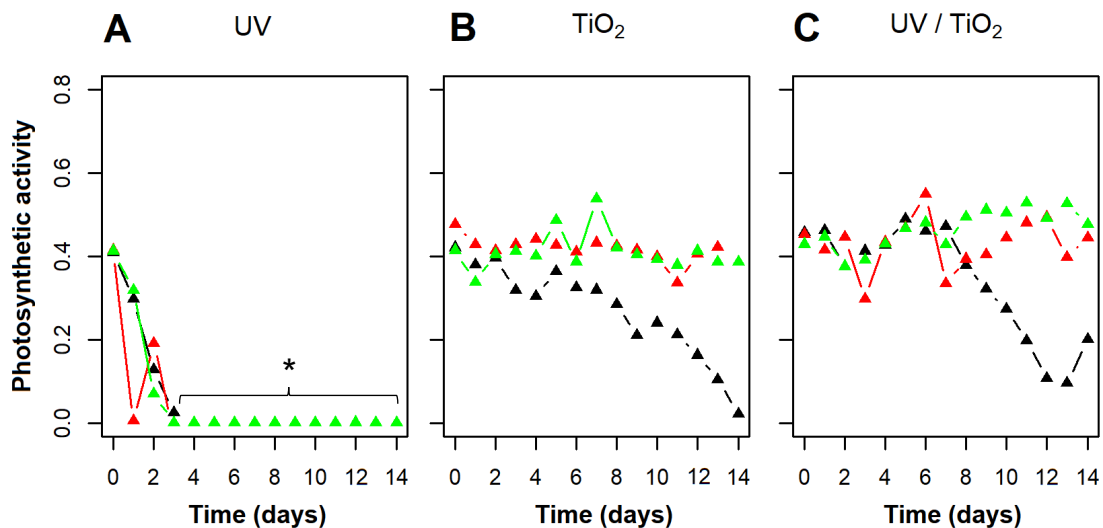
235 Biological replicates can commonly present different behaviors even when exposed to
 236 very similar conditions. *M. aeruginosa* PCC7813 cell numbers showed slightly different
 237 trends during TiO_2 -only treatment with variability increasing as the investigation
 238 progressed, particularly after day 10. The outlier observed on day 6 probably occurred
 239 due to lack of mixing during cell counting, since samples were consistent until day 10.
 240 *M. aeruginosa* PCC7813 cell numbers decreased on average from 5.8×10^6 to $2.6 \times$
 241 10^6 cells mL^{-1} with a significant rate of 0.19×10^6 cells $\text{mL}^{-1} \text{day}^{-1}$ ($p < 0.01$) over 14 days
 242 (Figure 1B) represented by linear regression (Figure S5). The variability that increased
 243 over time might have occurred due to adsorption of cells onto the surface of the TiO_2
 244 layer on the beads and to adhesion of cells onto the inside walls of the reactor.
 245 A reduction in cell numbers was expected to be observed in the UV/ TiO_2 treatment on
 246 the *M. aeruginosa* PCC7813 cell density based on previous bench-scale studies
 247 (Pestana *et al.*, 2020; Chang *et al.*, 2018; Song *et al.*, 2018; Wang *et al.*, 2018, 2017;
 248 Pinho *et al.*, 2012). However, the *M. aeruginosa* cell density could best be represented
 249 by a piecewise regression tendency (Figure S6) and significantly rose in the UV/ TiO_2

250 treatment over the first eight days with a tendency rate of 0.46×10^6 cells mL⁻¹ day⁻¹
251 ($p < 0.01$), and then decreased after day 8 with a tendency rate of 1×10^6 cells mL⁻¹ day⁻¹
252 ($p < 0.01$; Figure 1C). One possible explanation for this observation is that the TiO₂
253 coated glass beads have converted some of the incoming UV irradiation into visible
254 light through fluorescence from the semiconductor material (Li *et al.*, 2016) in sufficient
255 quantities to support modest growth, despite the fact that ambient overhead light was
256 of low intensity ($2.5 \mu\text{mol photons m}^{-2} \text{s}^{-1}$) and nominally insufficient for significant cell
257 growth evidenced by no growth observed in the treatments without LEDs (Figure 1B).
258 Photoluminescence measurements of the TiO₂ coated glass beads show that the
259 beads generate additional visible light, albeit with low efficiency of 7%. The spectrum
260 was generated at a wavelength of around 430 nm, presenting an overlap with the blue
261 absorption peak of chlorophyll *a*, which can be used by cyanobacteria since chlorophyll
262 *a* has a significant absorbance at this same wavelength and might have contributed to
263 growth of the cyanobacteria (supplementary material S5). It is possible that at the same
264 time cells were receiving sufficient light to grow, during UV/TiO₂ treatment, cells were
265 being damaged and growth was inhibited. Mathew *et al.* (2012) also observed
266 emission of new wavelengths in the range of visible light (387, 421, 485, 530 and 574
267 nm) from TiO₂ colloidal nanoparticles after the excitation wavelength of 274 nm. The
268 sample behavior after day 8 is not a true reflection of the individual replicates. After 8
269 days, the replicate treatments diverged with one of the replicates (Figure 1C: black)
270 declining rapidly (cell density decreased from 5.8×10^6 to 3.1×10^5 cells mL⁻¹), while
271 the two other replicates (Figure 1C: red and green) grew, with a cell density increasing
272 from 5.6×10^6 to 7.7×10^6 cells mL⁻¹ for one of these replicates (red) and from 5.6×10^6
273 to 8.9×10^6 cells mL⁻¹ in the other (green).

274 In order for the UV illumination to target a specific organism or to activate a catalyst, it
275 must be able to first transmit through the water (Summerfelt, 2003). The lack of cell
276 removal by photocatalysis in two out of three samples during the UV/TiO₂ treatment
277 could be explained by the air flow within the reactor design. In the UV/TiO₂

278 photocatalytic treatment, coated beads inside of the pods may have dispersed the
279 rising air flow into smaller air bubbles, thus attenuating the light to the point where an
280 insufficient number of photons reached the TiO₂ to produce hydroxyl radicals that would
281 be responsible for *M. aeruginosa* PCC7813 removal. The sparging pattern in the
282 reactor where photocatalytic removal of *M. aeruginosa* PCC7813 was observed may
283 have been such that permitted better light penetration, allowing the activation of TiO₂
284 coated beads by UV illumination and subsequent sufficient hydroxyl radical production.
285 Direct photolysis and the indirect oxidation by extracellular reactive oxygen species
286 (ROS) initially cause cellular stress and then damage to the cell membrane, without
287 promoting the complete destruction of the cell (Ou *et al.* 2011a, 2011b). Photosynthetic
288 activity as expressed as the F_V/F_M' ratio is a rapid method that can represent the level
289 of stress and/or damage in cyanobacterial cells (Menezes *et al.*, 2020; Stirbet *et al.*,
290 2018; Yang *et al.*, 2013). Cyanobacterial stress causes a decline in the F_V/F_M' ratio,
291 which means that the lower the F_V/F_M' ratio (photosynthetic activity) the more damage
292 or stress there is to the cyanobacteria. During the UV treatment, cyanobacterial cells
293 suffered inhibition of photosynthetic activity especially at the beginning of the
294 experiment from days 1 to 4 (Figure 2A). The photosynthetic activity decrease
295 observed during photolysis corresponds to the decrease in the cell number observed
296 until day 3 (Figure 1A). As previously reported by Menezes *et al.* (2020), photosynthetic
297 activity measurements showed a faster response to cell damage than cell density
298 measurements, indicating that cell stress occurred as early as 24 hours before cell
299 density changes could be observed by cell density measurements. The cell stress
300 results from day 3 are most likely due to the very low cell density observed from that
301 point in time (5×10^5 cells mL⁻¹), which were lower than the minimum concentration of
302 cells required for cell stress determination. For the TiO₂-only treatment photosynthetic
303 activity remained consistent for the first 6 days (Figure 2B), remaining at the same level
304 for two out of the three replicates until the end of 14 days (Figure 2B: red and green).
305 These results support the hypothesis from cell density observations (Figure 1B) that

306 cells were not inhibited or damaged but were removed from suspension and thus
 307 influencing the cell enumeration. Before carrying out the study, UV/TiO₂ treatment was
 308 expected to be the most effective treatment through damage to the photosynthetic
 309 system of *M. aeruginosa* PCC7813. However, relatively little effect was observed in the
 310 UV/TiO₂ treatment over the first 8 days with only one of the replicates showing a
 311 decline in photosynthetic activity from day 7 onwards (Figure 2C: black) which also
 312 corresponds to the cell density decrease in that replicate. (Figure 1C: black).
 313

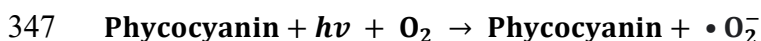


314 **Figure 2** – Effects of (A) UV-LED irradiation (365 nm), (B) TiO₂ coated glass beads under ambient light (2.5 μmol photons m⁻² s⁻¹) and (C) photocatalytic treatment on *Microcystis aeruginosa* PCC7813 photosynthetic activity using TiO₂ coated glass beads under UV-LED illumination (365 nm) over 14 days under sparging with sterile air. Data points represent individual replicates from each treatment. *Data points below the limit of quantification as too few cells remained for reliable quantification.

315
 316 An initial decrease of *M. aeruginosa* PCC7813 cell density at the beginning of the
 317 experiment was expected which was what had been observed previously in other
 318 studies that evaluated *M. aeruginosa* cell density after TiO₂ photocatalytic treatment
 319 (Pestana *et al.*, 2020; Chang *et al.*, 2018; Song *et al.*, 2018; Wang *et al.*, 2018, 2017;
 320 Pinho *et al.*, 2012). In particular, the study of Pestana *et al.* (2020), was a similar
 321 experimental design albeit in a smaller bench scale (30 mL of cell suspension and 700
 322 mg of coated beads, equivalent to 0.2% (w/v) TiO₂). The differences in results between

323 the two studies could be due to the light attenuation of the bubbles being dispersed by
324 the beads.

325 In the current study, photolysis by UV illumination (365 nm) was observed to be the
326 most effective treatment for *M. aeruginosa* PCC7813 cell destruction. The reduction in
327 the *M. aeruginosa* PCC7813 cell density (Figure 1A) might be explained by the fact that
328 cyanobacteria do not produce sufficient ROS-scavenging enzymes (e.g., ROS
329 produced by UV treatment; Sinha *et al.*, 2018). ROS oxidize lipids and proteins inside
330 the cyanobacterial cells, resulting in cell wall damage, followed by inactivation of
331 enzymes and ultimately cell death (Sinha *et al.*, 2018). Furthermore, the effect of the
332 UV treatment on *M. aeruginosa* PCC7813 cells might have been caused by indirect
333 oxidation due to intracellular ROS (Ou *et al.* 2011a, 2011b). Intracellular ROS
334 generation may have been enhanced by the presence of intracellular phycocyanin
335 which is a natural cyanobacterial pigment (Robertson *et al.*, 1999). Robertson *et al.*
336 (1999) suggested that cell destruction can occur from the inside-out rather than the
337 outside-in due to the production of both singlet oxygen and hydroperoxide radical
338 facilitated by the intracellular phycocyanin upon UV-irradiation. After this, the
339 intracellular ROS effects on cells were enhanced by phycocyanin, causing complete
340 degradation of cells. Under UV illumination alone, phycocyanin can contribute to the
341 degradation of cells by two mechanisms: firstly, during the electron transfer process
342 (Equation 1), the photoexcited phycocyanin transfers an electron to oxygen, producing
343 the superoxide radical that then becomes a hydroperoxide radical by protonation.
344 Secondly, during the energy transfer process (Equation 2), phycocyanin and oxygen
345 interact to produce singlet oxygen (Robertson *et al.*, 1999) with both ROS attacking the
346 cell structures from within.



350 Furthermore, cyanobacteria release oxygen during photosynthesis which can interact

351 with UV light and other organic compounds to produce ROS (Pattanaik *et al.*, 2007).
352 The ROS produced by UV-A illumination in the present study might also be responsible
353 for damaging *M. aeruginosa* PCC7813 cells.
354 UV-C (254 nm) has been widely applied as a germicide for the inactivation of bacteria
355 and viruses by denaturing the DNA of microorganisms and causing death or function
356 loss (Boyd *et al.*, 2020; Summerfelt, 2003). However, it is likely that the UV-A
357 illumination (365 nm) used in the present study was able to destroy *M. aeruginosa*
358 PCC7813 cells due to the generation of ROS and the presence of phycocyanin inside
359 the cyanobacterial cells. Therefore, unlike UV-C illumination, UV-A illumination might be
360 specific to cyanobacterial control and it may not affect other phytoplankton such as
361 diatoms or green algae, although this requires further confirmation. The specificity of
362 the effects of the UV-A photolysis on cyanobacteria would impact the phytoplankton
363 community in natural waterbodies less than the application of UV-B/UV-C photolysis. At
364 the same time, having the additional advantage of presenting with lower capital cost.
365 Previous studies have investigated the application of other treatments (e.g., hydrogen
366 peroxide oxidation) and observed that some treatment were selective for
367 cyanobacterial species due to their biochemistry (Drábková *et al.*, 2007a; Drábková *et*
368 *al.*, 2007b; Matthijs *et al.*, 2012). Ou *et al.* (2011a, 2011b) pointed out that the UV-C-
369 induced damage occurs via either direct photolysis or indirect oxidation by intra- and/or
370 extracellular ROS. UV irradiation causes damage to the photosynthesis system,
371 including PS I, PS II and phycobilisome which interrupts the electron transport chain
372 and retards the critical reactions during photosynthesis, followed by the decomposition
373 of cytoplasmic inclusions and finally cell destruction with release of intracellular organic
374 matter. The same mechanisms might have occurred during the present UV-A photolysis
375 where the photosynthetic system of *M. aeruginosa* PCC7813 was affected (Figure 2A)
376 and cellular destruction occurred due to intracellular ROS (Figure 1A). Yang *et al.*
377 (2015) evaluated the effects of high-energy UV-B illumination (280–320 nm) on a toxic
378 (FACHB 915) and a non-toxic (FACHB 469) strain of *M. aeruginosa* photosynthetic

379 activity. The UV-B irradiation resulted in an inhibition of the photosynthetic activity of
380 both toxic and non-toxic strains over 3 days of exposure due to damage to
381 photosystem II (Yang *et al.*, 2015). However, both *M. aeruginosa* strains used by Yang
382 *et al.* (2015) showed signs of photosynthetic activity recovery at the end of the
383 experiment.

384

385 **3.2 Intra- and extracellular microcystin removal**

386 The intracellular microcystin concentration for all analogues diminished significantly in
387 a piecewise regression tendency (Figure S7 – S10) over the first 5 days of the UV
388 treatment (Figure 3A) with the complete removal of all microcystin analogues by this
389 time (approximate rate of 40, 22, 15 and 2.6 ng mL⁻¹ day⁻¹ of intracellular MC-LR, MC-
390 LF, MC-LW and MC-LY, respectively, $p < 0.01$ for all samples). The decrease of all four
391 analogues of intracellular microcystins during UV treatment (Figure 3A) corresponds to
392 the reduction of *M. aeruginosa* cell density and subsequent microcystins leak (Figure
393 1A). For the TiO₂-only samples (Figure 3B), the mean values suggest removal of 20,
394 43, 42 and 42% of intracellular MC-LR, MC-LF, MC-LW and MC-LY, respectively, or a
395 significant decrease in a linear regression rate (Figure S11 – S14) of 3.7, 2.8, 2.9 and
396 0.3 ng mL⁻¹ day⁻¹ (for all samples $p < 0.05$) over 14 days. Samples remained consistent
397 over the first 11 days, however, it was possible to observe divergence in the results in
398 the later stages. During UV/TiO₂ treatment, intracellular microcystins samples
399 presented high variability over 14 days (Figure 3C) and while one replicate (Figure 3C:
400 black) showed complete removal of all microcystins at the end of the experiment,
401 another replicate (Figure 3C: green) demonstrated microcystins concentration of 157,
402 74, 59 and 11 ng mL⁻¹ for MC-LR, MC-LF, MC-LW and MC-LY respectively. It is
403 noteworthy that across all the treatments all microcystin analogues behaved in a similar
404 manner (Figure 3), for example, one replicate during the UV treatment (Figure 3A: red)
405 all analogues decreased on day 2, followed by the other two replicates on day 4
406 (Figure 3A: green and black). Variability in the toxin concentrations observed in Figure

407 3C is a further indication that both cell lysis due to UV/TiO₂ and cell growth due to the
408 production of visible light are acting in the system.

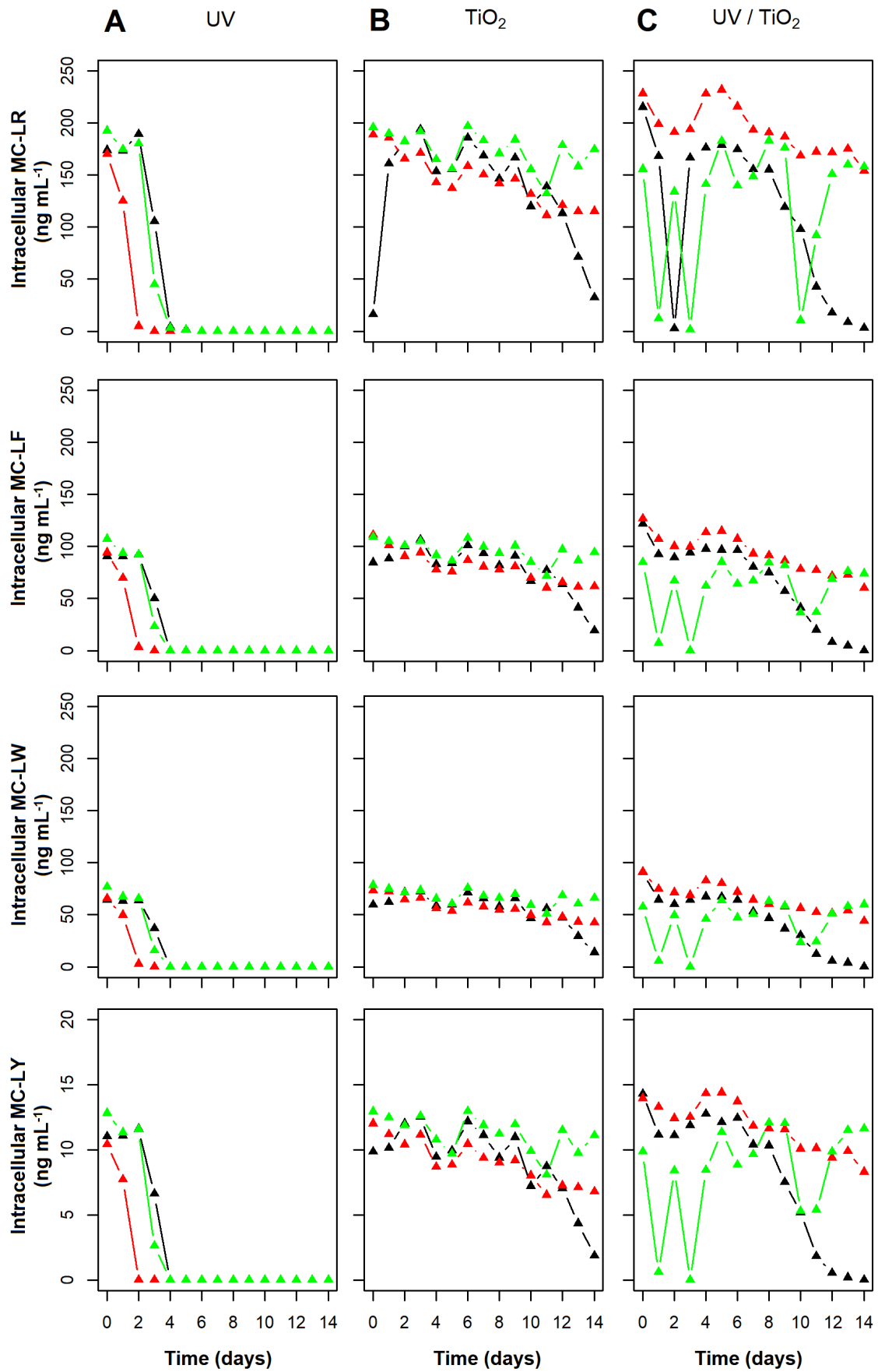
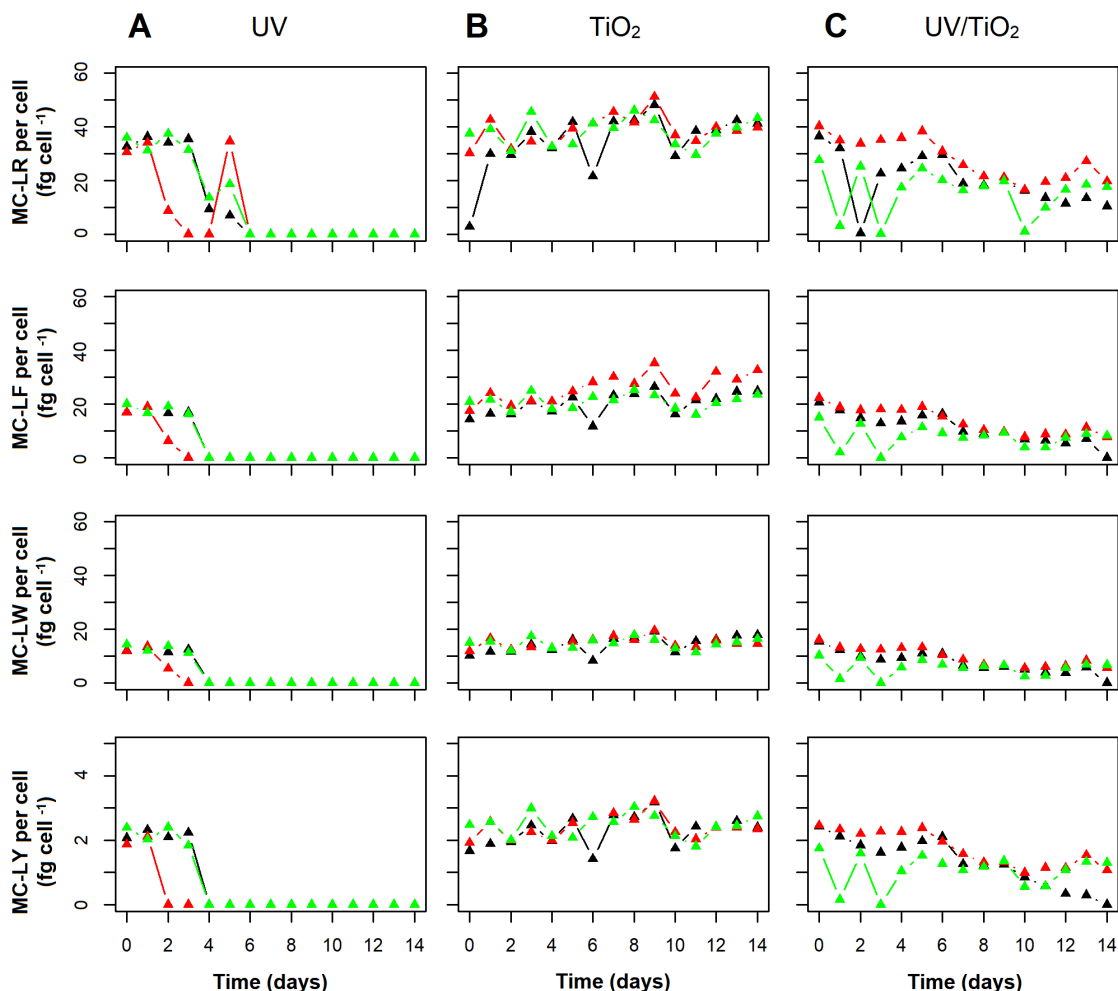


Figure 3 – Intracellular microcystin concentrations produced by *Microcystis aeruginosa* PCC7813 during (A) UV, (B) TiO₂ under ambient light (2.5 μmol photons m⁻² s⁻¹) and (C) UV/TiO₂ treatment over 14 days under constant agitation. Data points represent individual replicates from each treatment.

410



411

Figure 4 – Intracellular microcystin analogues ratio (toxin cell⁻¹) in *Microcystis aeruginosa* PCC7813 over 14 days of (A) UV, (B) TiO₂ under ambient light (2.5 μmol photons m⁻² s⁻¹) and (C) UV/TiO₂ treatment under constant agitation. Data points represent individual replicates from each treatment.

412

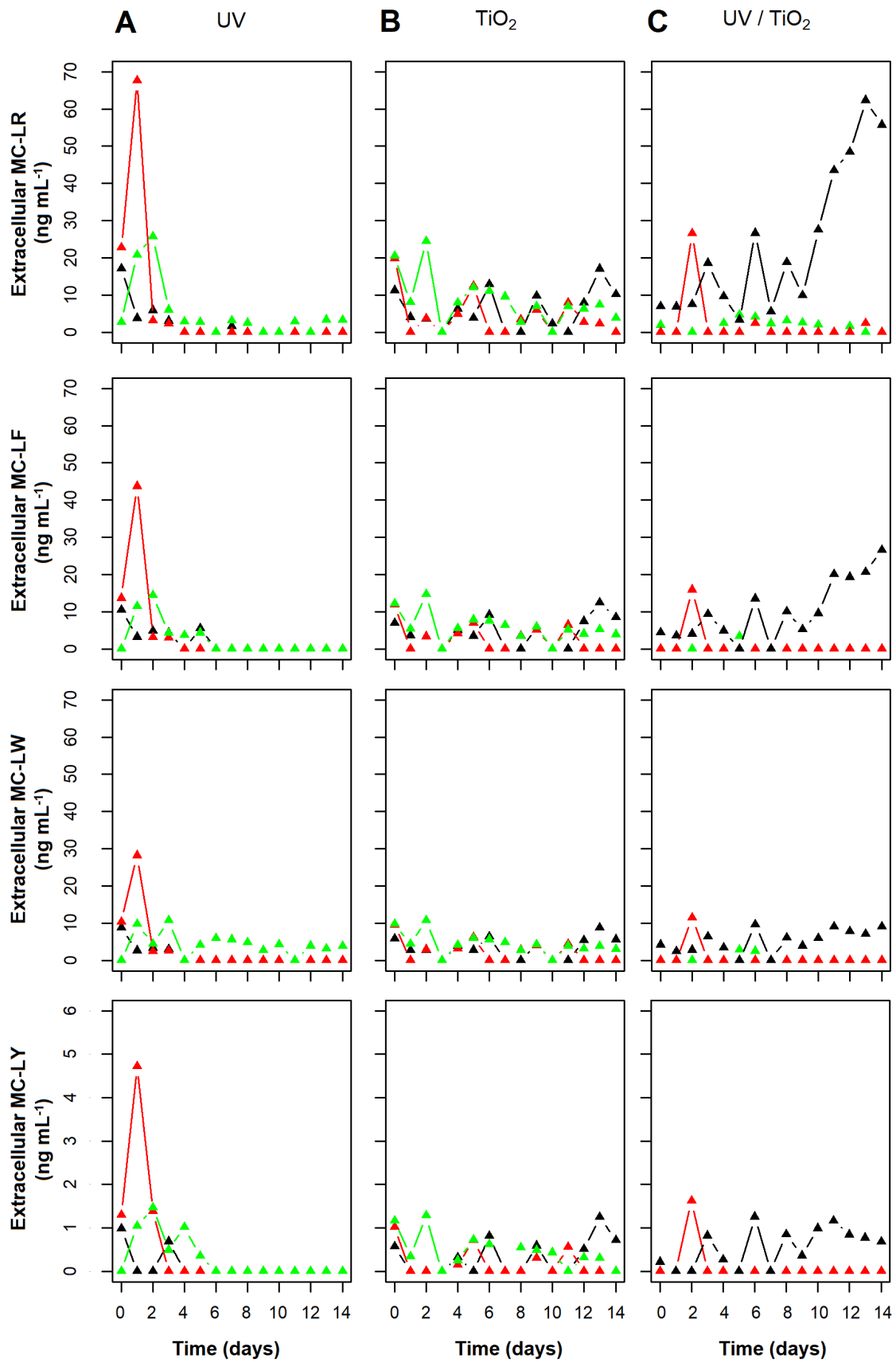
413 For the UV treatment, all microcystins per cell were undetectable after 6 days (Figure
 414 4A). The complete destruction of cells during photolysis (Figure 1A) could be confirmed
 415 by this corresponding decrease in the toxin ratio (i.e., toxin concentration per cell
 416 number). For TiO₂-only samples, the toxin concentration per cell presented variability
 417 (Figure 4B). Despite the slight decrease in cell number of TiO₂-only samples, no cell
 418 stress was detected when analyzing both photosynthetic activity (Figure 2B) and

419 intracellular toxin (Figure 3B), indicating that cells were not actually damaged and/or
420 dead but there was physical cell removal of intact healthy cells by adsorption of cells
421 onto the surface of the TiO₂ beads and the surface of the reactors.

422 The amount of toxin per cell over 14 days in the UV/TiO₂ treatment diminished by 54,
423 64, 70 and 72% for MC-LR, -LY, -LW and -LF, respectively (Figure 4C). One reason for
424 the reduction in the toxin concentration per cell could be that some of the *M.*
425 *aeruginosa* PCC7813 cells were detected and counted as living organisms, however,
426 some of the cells were probably fragmented and inactive. Additionally, as was
427 previously mentioned, intracellular microcystin could leak the cell if the cell wall was
428 compromised. Another reason for the decrease in toxin concentration could be
429 microcystins binding to intracellular proteins which *M. aeruginosa* is known to do as
430 demonstrated by Zilliges *et al.* (2011). Pestana *et al.* (2020) also observed a reduction
431 in the toxin per cell ratio of the same intracellular microcystin analogues used in the
432 present study (MC-LR, -LY, -LW and -LF) TiO₂ coated glass beads under UV/LED
433 illumination (365 nm, 2.1 mW s⁻¹), which they ascribed to microcystins binding to
434 intracellular proteins.

435 Microcystins are commonly released into the surrounding water after cell rupture by
436 water treatment processes. Therefore, water treatment technologies must be applied to
437 remove toxins that are released into the water since conventional treatment cannot
438 remove dissolved components (Chow *et al.*, 1999). After the liberation of intracellular
439 microcystins during the UV treatment, samples could be best represented by a
440 piecewise regression (Figure S19 – S22) with removal for all extracellular microcystins
441 amounting to 92% for MC-LR and complete removal of the other three analogues over
442 the first 5 days (Figure 5A). The reduction in *M. aeruginosa* PCC7813 cell number
443 (Figure 1A) is the most likely reason for the decrease of intracellular microcystins
444 during the UV treatment (Figure 3A) due to cell lysis and release of the intracellular
445 content to the surrounding water followed by the immediate removal of the extracellular
446 microcystins by direct photolysis and indirect oxidation of ROS (Figure 5A). No

447 significant change ($p>0.05$) in the extracellular concentration of any of the microcystin
448 analogues was observed over 14 days in the TiO₂-only samples (Figure 5B), indicating
449 that there was no microcystins release from the cells. This finding also corroborates the
450 theory that cells were not destroyed in TiO₂-only samples and remained intact. During
451 UV/TiO₂ treatment, there was no increase in the extracellular microcystin
452 concentrations for most samples over 14 days (Figure 5C: red and green). However,
453 the cell reduction observed for one of the replicates (Figure 2C: black) and the decline
454 of intracellular microcystins (Figure 3C: black) of this replicate in the UV/TiO₂ treatment
455 could account for the increase of extracellular microcystins (Figure 5C: black). The
456 toxin concentration released in this replicate (Figure 5C: black) corresponds to the
457 concentration increase of the extracellular microcystins, an indication of cell lysis
458 caused by the UV/TiO₂.
459



460

Figure 5 – Extracellular microcystin analogue concentrations produced by *Microcystis*

aeruginosa PCC7813 during (A) UV, (B) TiO₂ under ambient light (2.5 μmol photons m⁻² s⁻¹) and (C) UV/TiO₂ treatment over 14 days under constant agitation. Data points represent individual replicates from each treatment.

461

462 A study by Robertson *et al.* (1999) evaluated the destruction of MC-LR under UV/TiO₂
463 photocatalysis and photolysis in the presence of phycocyanin. The authors also
464 observed a decline of MC-LR concentration when the sample was treated with only UV-
465 A light in the presence of phycocyanin, corroborating the results of the current study.
466 However, when no phycocyanin was present, the UV light had no effect on the toxin
467 degradation, showing that phycocyanin acts as a photocatalyst for microcystin
468 destruction under UV illumination until the pigment was completely bleached
469 (Robertson *et al.*, 1999). There is a number of studies which have investigated the
470 effects of UV illumination on microcystins (Liu *et al.*, 2010; Pinho *et al.*, 2015a, 2015b,
471 2012; Triantis *et al.*, 2012), however, the breakdown of pure microcystin requires UV-C.
472 In order for the UV-A illumination used in the current study to breakdown microcystins,
473 the presence of phycocyanin is necessary. Similar effects were observed by Rinalducci
474 *et al.* (2008) which demonstrated the photosensitizing effect of phycocyanin on the
475 phycobilisomes of another cyanobacterium (*Synechocystis* PCC 6803).
476 Pestana *et al.* (2020) carried out a bench-scale (30 mL of cell suspension) study of the
477 destruction *M. aeruginosa* strain (PCC7813) (MC-LR, -LY, -LF and -LW) under UV/TiO₂
478 photocatalysis the TiO₂ coated beads used in the current study. Intracellular microcystin
479 analogues were removed by 49% and extracellular microcystins that were release after
480 cell lysis were completely removed by UV/TiO₂ photocatalysis. Similar results were
481 expected in the current study, however, UV photolysis was more efficient for the
482 removal of microcystins than the UV/TiO₂ photocatalytic treatment used in the present
483 study. The difference in the results might have occurred due to the larger scale and
484 lower initial cell concentration (6.5 L with 5 x 10⁶ cells mL⁻¹ in the current study
485 compared to 30 mL with 15 x 10⁶ cells mL⁻¹ used in Pestana *et al.* (2020) study).
486 Further, in the current study, a small amount of cell growth was observed in UV/TiO₂

487 treatment over the first 8 days (Figure 1C). Additionally, stronger mixing caused by the
488 multi-porous air-stone in the base of the reactor in the current study combined with the
489 dispersion of the larger air bubbles by the TiO₂-coated glass beads that potentially
490 attenuated the effects of the UV irradiation, rendering the UV/TiO₂ treatment less
491 effective. In contrast, in the Pestana *et al.* (2020) study, only very gentle single point
492 sparging (flow rate of 1.5 L min⁻¹) was used from the top of the vials. Finally, the
493 shadowing effect caused by the coated glass beads and the stainless-steel pods inside
494 the reactors (which were not used in the Pestana *et al.* (2020) study) may have
495 interfered in the efficiency of the photocatalytic removal of the microcystins.

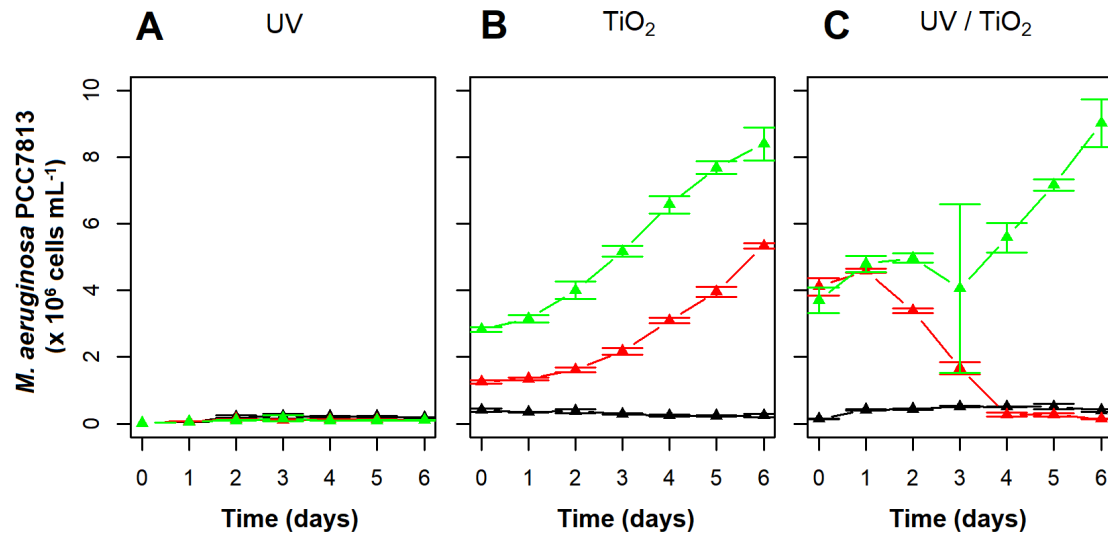
496

497 **3.3 *Microcystis aeruginosa* PCC7813 regrowth post UV and UV/TiO₂ treatment**

498 It is important to evaluate cyanobacterial regrowth potential to determine the residual
499 effects of the treatment. For the UV-A treated cells the difference in cell concentration
500 between the beginning of the regrowth experiment and day 6 was not significant
501 ($p=0.08$) due to the fact that few cells remained viable after UV treatment that were not
502 inhibited/damaged (Figure 6A). The remaining *M. aeruginosa* PCC7813 cells had a
503 doubling rate of 1.9 days over 6 days of regrowth (Figure 6A), which is still considered
504 a typical doubling rate for *M. aeruginosa*. For the TiO₂-only samples, variability was
505 high, with one of the replicates (Figure 6B: black) which had the lowest cell density
506 after 14 days treatment with TiO₂-only showing no regrowth. This replicate (Figure 6B:
507 black) actually showed a decreased in cell density from 4.1×10^5 to 2.5×10^5 cells mL⁻¹
508 over 6 days, while the other two replicates (Figure 6B: red and green) presented a
509 doubling rate of 2.9 and 3.8 days, respectively. The same sample variability was
510 observed in regrowth samples from the UV/TiO₂ treatment (Figure 6C). While cell
511 concentrations in two replicates (Figure 6C: black and green) doubled at a rate of 4.2
512 and 4.7 days respectively, the third replicates (Figure 6C: red) decreased in cell density
513 from 4.1×10^6 to 1.4×10^5 cells mL⁻¹ over 6 days.

514 Wilson *et al.* (2006) stated an average doubling rate for 32 strains of *Microcystis*

515 cultured in BG-11 medium as 2.8 days. Some UV treatment samples from the current
516 study presented a faster doubling rate of 1.9 days and some UV/TiO₂ treatment
517 samples showed a slower doubling rate of 4.2 and 4.7 days.
518 Despite the lower initial cell density after 6 days of regrowth in UV treatment (Figure
519 6A), the cells in UV treatment showed the fastest doubling rate (1.9 days) when
520 compared to cells from TiO₂-only samples and UV/TiO₂ treatment (Figures 6B and C),
521 as previously observed by Dunn and Manoylov (2016). In the UV treatment, low cell
522 density means low competition for resources, hence this is often when growth is
523 fastest.
524



525

Figure 6 – Effects of (A) UV-LED irradiation (365 nm), (B) TiO₂ coated glass beads under ambient light (2.5 μmol photons m⁻² s⁻¹) and (C) photocatalytic treatment on *Microcystis aeruginosa* PCC7813 regrowth using TiO₂ coated glass beads under UV-LED illumination (365 nm) over seven days under cool white fluorescent lights of 10.5 μmol photons m⁻² s⁻¹. Data points represent the average of four replicates from each treatment where four individual vials were used for samples of each tested system (UV-only, TiO₂-only and UV/TiO₂) to assess regrowth ($n = 4$).

526

527 Ou *et al.* (2012) studied the effects of different UV-C dosages (140-4200 mJ cm⁻²) on
 528 *M. aeruginosa* FACHB-912 recovery over 7 days. They found a significant reduction in
 529 indicators of photosynthesis (e.g., quantum yield) and chlorophyll a for samples
 530 irradiated at 350, 700, 1400 and 4200 mJ cm⁻², showing the irreversible inhibition of the
 531 photosynthetic system in the *M. aeruginosa* cells FACHB-912 after UV-C irradiation
 532 which then inhibited the reproduction and recovery of *M. aeruginosa* cells (Ou *et al.*,
 533 2012).

534 A study by Huang *et al.* (2011) evaluated the regrowth potential of *M. aeruginosa* after
 535 24 hours of ZnO/γ-Al₂O₃ photocatalytic treatment under solar light. After 12 days of
 536 regrowth, the cell density of treated samples was less than 85% of that of the control,
 537 highlighting the lasting effect of photocatalysis on *M. aeruginosa* cells even though a

538 different type of photocatalyst and irradiation was applied (Huang *et al.*, 2011).

539

540 **4 Conclusion**

541 The current study investigated the effects of UV-A photolysis and a UV/TiO₂
542 photocatalytic system using TiO₂ coated glass beads on *M. aeruginosa* PCC7813 cells
543 and the four main microcystin analogues (MC-LR, -LY, -LW and -LF) this strain
544 produces. Both systems had energy-efficient UV illumination supplied by UV-LEDs for
545 cyanobacteria and cyanotoxin control. The UV photolysis was able to consistently
546 remove cyanobacterial cells and toxins, and therefore was shown to be more effective
547 than the UV/TiO₂ photocatalytic system which gave a delayed removal of cells and
548 concerningly, slightly supported growth in the first 8 days. All the data analysis (cell
549 density, photosynthetic activity, toxin per cell, intra- and extracellular toxin) indicate that
550 UV-A photolysis was capable of not only inhibiting *M. aeruginosa* PCC7813 cells, but it
551 significantly damaged them to the point that only a very limited regrowth was observed.
552 An advantage of using UV-A irradiation over other types of UV irradiation is that UV-A
553 illumination might be specific to cyanobacterial control due to the presence of
554 phycocyanin inside of the cyanobacterial cells. To confirm this, the effects of UV
555 photolysis on other phytoplankton (diatoms and green algae) and cyanobacterial
556 species should be investigated, such as a mesocosms experiment with community
557 analysis. An additional advantage of employing UV-A over other types of UV irradiation
558 is that lamps generating UV-A tend to be more economical in terms of capital cost
559 compared to UV-B or UV-C generating lamps. In practice, many aspects of the reactor
560 design need to be optimized and field-tested to allow *in-situ* application inside
561 reservoirs: vertical or horizontal orientation of reactors, optimization of the active
562 surface area and contact time, incorporation of waterproof UV-LEDs, and powering the
563 units *in-situ* exploring solar options. The current study has successfully demonstrated
564 that UV-LED-based advanced oxidation techniques could be operated at a larger-than-

565 bench scale and control cyanobacteria and their toxins.

566

567 **5 Acknowledgements**

568 The authors would like to thank the Engineering and Physical Sciences Research

569 Council (EPSRC) [EP/P029280/1], the Coordination for the Improvement of

570 Higher Education Personnel - CAPES [PROEX 20/2016 and PrInt

571 88887.311806/2018-00], and the Brazilian National Research Council – CNPq

572 [403116/2016-3 and 304164/2017-8] for funding this research. As per EPSRC

573 requirement all data will be made publicly available via the Robert Gordon

574 University's open access repository OpenAIR@RGU. Further, the first author

575 also acknowledges the scholarship from the Brazilian National Research Council

576 - CNPq. Finally, Len Montgomery is appreciated for proof-reading the manuscript

577 and the authors would like to thank Dr Nathan Skillen of Queen's University

578 Belfast, for help and guidance with the electrical wiring of the LEDS for the

579 reactors.

580

581 **6 References**

582 Akkanen, J., Kukkonen, J.V.K., 2003. Measuring the bioavailability of two hydrophobic
583 organic compounds in the presence of dissolved organic matter. *Environ. Toxicol.*
584 *Chem.* 22, 518–524.

585 Boyd, B., Suslov, S.A., Becker, S., Greentree, A.D., Maksymov, I.S., 2020. Beamed UV
586 sonoluminescence by aspherical air bubble collapse near liquid-metal
587 microparticles. *Sci. Rep.* 10, 1–8. <https://doi.org/10.1038/s41598-020-58185-2>

588 Carmichael, W.W., Azevedo, S.M.F.O., An, J.S., Molica, R.J.R., Jochimsen, E.M., Lau,
589 S., Rinehart, K.L., Shaw, G.R., Eaglesham, G.K., 2001. Human fatalities from
590 cyanobacteria: Chemical and biological evidence for cyanotoxins. *Environ. Health*
591 *Perspect.* 109, 663–668. <https://doi.org/10.1289/ehp.01109663>

592 Chae, S., Noeiaghahi, T., Oh, Y., Kim, I.S., Park, J.S., 2019. Effective removal of
593 emerging dissolved cyanotoxins from water using hybrid photocatalytic composites.
594 *Water Res.* 149, 421–431. <https://doi.org/10.1016/j.watres.2018.11.016>

- 595 Chang, C.W., Huo, X., Lin, T.F., 2018. Exposure of *Microcystis aeruginosa* to hydrogen
596 peroxide and titanium dioxide under visible light conditions: Modeling the impact of
597 hydrogen peroxide and hydroxyl radical on cell rupture and microcystin degradation.
598 Water Res. 141, 217–226. <https://doi.org/10.1016/j.watres.2018.05.023>
- 599 Chen, L., Zhao, C., Dionysiou, D.D., O'Shea, K.E., 2015. TiO₂ photocatalytic degradation
600 and detoxification of cylindrospermopsin. J. Photochem. Photobiol. A Chem. 307–
601 308, 115–122. <https://doi.org/10.1016/j.jphotochem.2015.03.013>
- 602 Chow, C.W.K., Drikas, M., House, J., Burch, M.D., Velzeboer, R.M.A., 1999. The impact
603 of conventional water treatment processes on cells of the cyanobacterium
604 *Microcystis aeruginosa*. Water Res. 33, 3253–3262. <https://doi.org/10.1016/S0043->
605 1354(99)00051-2
- 606 Drábková, Michaela, Admiraal, W., Maršálek, B., 2007a. Combined exposure to
607 hydrogen peroxide and light-selective effects on cyanobacteria, green algae, and
608 diatoms. Environ. Sci. Technol. 41, 309–314. <https://doi.org/10.1021/es060746i>
- 609 Drábková, M., Matthijs, H.C.P., Admiraal, W., Maršálek, B., 2007b. Selective effects of
610 H₂O₂ on cyanobacterial photosynthesis. Photosynthetica 45, 363–369.
611 <https://doi.org/10.1007/s11099-007-0062-9>
- 612 Dunn, R.M., Manoylov, K.M., 2016. The Effects of Initial Cell Density on the Growth and
613 Proliferation of the Potentially Toxic Cyanobacterium *Microcystis aeruginosa* J.
614 Environ. Prot. (Irvine, Calif). 07, 1210–1220.
615 <https://doi.org/10.4236/jep.2016.79108>
- 616 Falconer, I.R., Beresford, A.M., Runnegar, M.T.C., 1983. Evidence of liver damage by
617 toxin from a bloom of the blue-green alga, *Microcystis aeruginosa*. Med. J. Aust. 1,
618 511–514. <https://doi.org/10.5694/j.1326-5377.1983.tb136192.x>
- 619 Fan, F., Shi, X., Zhang, M., Liu, C., Chen, K., 2019. Comparison of algal harvest and
620 hydrogen peroxide treatment in mitigating cyanobacterial blooms via an *in situ*
621 mesocosm experiment. Sci. Total Environ. 694, 133721.
622 <https://doi.org/10.1016/j.scitotenv.2019.133721>
- 623 Heering, W., 2004. UV-sources - Basics, Properties and Applications. Int. Ultrav. Assoc.
624 6, 7–13.
- 625 Hu, Xi, Hu, Xinjiang, Tang, C., Wen, S., Wu, X., Long, J., Yang, X., Wang, H., Zhou, L.,
626 2017. Mechanisms underlying degradation pathways of microcystin-LR with doped
627 TiO₂ photocatalysis. Chem. Eng. J. 330, 355–371.
628 <https://doi.org/10.1016/j.cej.2017.07.161>

- 629 Huang, W.J., Lin, T.P., Chen, J.S., Shih, F.H., 2011. Photocatalytic inactivation of
630 cyanobacteria with ZnO/ γ -Al₂O₃ composite under solar light. J. Environ. Biol. 32,
631 301–307.
- 632 Hui, J., Pestana, C.J., Caux, M., Gunaratne, H.Q.N., Edwards, C., Robertson, P.K.J.,
633 Lawton, L.A., Irvine, J.T.S., 2021. Graphitic-C₃N₄ coated floating glass beads for
634 photocatalytic destruction of synthetic and natural organic compounds in water
635 under UV light. J. Photochem. Photobiol. A Chem. 405, 112935.
636 <https://doi.org/10.1016/j.jphotochem.2020.112935>
- 637 Jin, Y., Zhang, S., Xu, H., Ma, C., Sun, J., Li, H., 2019. Application of N-TiO₂ for visible-
638 light photocatalytic degradation of *Cylindrospermopsis raciborskii*. More difficult
639 than that for photodegradation of *Microcystis aeruginosa*?. Environ. Pollut. 245,
640 642–650. <https://doi.org/10.1016/j.envpol.2018.11.056>
- 641 Jochimsen, E., Carmichael, W.W., An, J., Cardo, D.M., Cookson, S.T.; Holmes, C.E.M.;
642 Antunes, B.C.; Melo Filho, D.A.; Lyra, T.M.; Barreto, V.S.T; Azevedo, S.M.F.O. &
643 Jarvis, W., 1998. Liver failure and death after exposure to microcystins. N. Engl. J.
644 Med. 338, 873–878. <https://doi.org/10.1080/13504509.2013.856048> M4 - Citavi
- 645 Li, L., Sahi, S.K., Peng, M., Lee, E.B., Ma, L., Wojtowicz, J.L., Malin, J.H., Chen, W.,
646 2016. Luminescence-and nanoparticle-mediated increase of light absorption by
647 photoreceptor cells: Converting UV light to visible light. Sci. Rep. 6.
648 <https://doi.org/10.1038/srep20821>
- 649 Liu, X., Chen, Z., Zhou, N., Shen, J., Ye, M., 2010. Degradation and detoxification of
650 microcystin-LR in drinking water by sequential use of UV and ozone. J. Environ. Sci.
651 22, 1897–1902. [https://doi.org/10.1016/S1001-0742\(09\)60336-3](https://doi.org/10.1016/S1001-0742(09)60336-3)
- 652 Mathew, S., Kumar Prasad, A., Benoy, T., Rakesh, P.P., Hari, M., Libish, T.M.,
653 Radhakrishnan, P., Nampoori, V.P.N., Vallabhan, C.P.G., 2012. UV-visible
654 photoluminescence of TiO₂ nanoparticles prepared by hydrothermal method. J.
655 Fluoresc. 22, 1563–1569. <https://doi.org/10.1007/s10895-012-1096-3>
- 656 Matthijs, H.C.P., Visser, P.M., Reeze, B., Meeuse, J., Slot, P.C., Wijn, G., Talens, R.,
657 Huisman, J., 2012. Selective suppression of harmful cyanobacteria in an entire lake
658 with hydrogen peroxide. Water Res. 46, 1460–1472.
659 <https://doi.org/10.1016/j.watres.2011.11.016>
- 660 Menezes, I., Maxwell-mcqueeney, D., Pestana, C.J., Edwards, C., Lawton, L.A., 2020.
661 Oxidative stress in the cyanobacterium *Microcystis aeruginosa* PCC 7813:
662 Comparison of different analytical cell stress detection assays. Chemosphere 269

663 128766. <https://doi.org/10.1016/j.chemosphere.2020.128766>

664 Moon, B.R., Kim, T.K., Kim, M.K., Choi, J., Zoh, K.D., 2017. Degradation mechanisms of
665 Microcystin-LR during UV-B photolysis and UV/H₂O₂ processes: Byproducts and
666 pathways. *Chemosphere* 185, 1039–1047.
667 <https://doi.org/10.1016/j.chemosphere.2017.07.104>

668 Ou, H., Gao, N., Deng, Y., Qiao, J., Wang, H., 2012. Immediate and long-term impacts
669 of UV-C irradiation on photosynthetic capacity, survival and microcystin-LR release
670 risk of *Microcystis aeruginosa*. *Water Res.* 46, 1241–1250.
671 <https://doi.org/10.1016/j.watres.2011.12.025>

672 Ou, H., Gao, N., Deng, Y., Qiao, J., Zhang, K., Li, T., Dong, L., 2011a. Mechanistic studies
673 of *Microcystis aeruginosa* inactivation and degradation by UV-C irradiation and
674 chlorination with poly-synchronous analyses. *DES* 272, 107–119.
675 <https://doi.org/10.1016/j.desal.2011.01.014>

676 Ou, H., Gao, N., Deng, Y., Wang, H., Zhang, H., 2011b. Inactivation and degradation of
677 *Microcystis aeruginosa* by UV-C irradiation. *Chemosphere* 85, 1192–1198.
678 <https://doi.org/10.1016/j.chemosphere.2011.07.062>

679 Pattanaik, B., Schumann, R., Karsten, U., 2007. Effects of Ultraviolet Radiation on
680 Cyanobacteria and Their Protective Mechanisms. *Limnology* 29–45.

681 Pestana, C.J., Capelo-Neto, J., Lawton, L., Oliveira, S., Carloto, I., Linhares, H.P., 2019.
682 The effect of water treatment unit processes on cyanobacterial trichome integrity.
683 *Sci. Total Environ.* 659, 1403–1414. <https://doi.org/10.1016/j.scitotenv.2018.12.337>

684 Pestana, C.J., Portela Noronha, J., Hui, J., Edwards, C., Gunaratne, H.Q.N., Irvine,
685 J.T.S., Robertson, P.K.J., Capelo-Neto, J., Lawton, L.A., 2020. Photocatalytic
686 removal of the cyanobacterium *Microcystis aeruginosa* PCC7813 and four
687 microcystins by TiO₂ coated porous glass beads with UV-LED irradiation. *Sci. Total*
688 *Environ.* 745, 141154. <https://doi.org/10.1016/j.scitotenv.2020.141154>

689 Pinho, L.X., Azevedo, J., Brito, A., Santos, A., Tamagnini, P., Vilar, V.J.P., Vasconcelos,
690 V.M., Boaventura, R.A.R., 2015a. Effect of TiO₂ photocatalysis on the destruction of
691 *Microcystis aeruginosa* cells and degradation of cyanotoxins microcystin-LR and
692 cylindrospermopsin. *Chem. Eng. J.* 268, 144–152.
693 <https://doi.org/10.1016/j.cej.2014.12.111>

694 Pinho, L.X., Azevedo, J., Miranda, S.M., Ângelo, J., Mendes, A., Vilar, V.J.P.,
695 Vasconcelos, V., Boaventura, R.A.R., 2015b. Oxidation of microcystin-LR and
696 cylindrospermopsin by heterogeneous photocatalysis using a tubular photoreactor

697 packed with different TiO₂ coated supports. Chem. Eng. J. 266, 100–111.
698 <https://doi.org/10.1016/j.cej.2014.12.023>

699 Pinho, L.X., Azevedo, J., Vasconcelos, V.M., Vilar, V.J.P., Boaventura, R.A.R., 2012.
700 Decomposition of *Microcystis aeruginosa* and microcystin-LR by TiO₂ oxidation
701 using artificial UV light or natural sunlight. J. Adv. Oxid. Technol. 15, 98–106.
702 <https://doi.org/10.1515/jaots-2012-0111>

703 Rinalducci, S., Pedersen, J.Z., Zolla, L., 2008. Generation of reactive oxygen species
704 upon strong visible light irradiation of isolated phycobilisomes from *Synechocystis*
705 PCC 6803. Biochim. Biophys. Acta - Bioenerg. 1777, 417–424.
706 <https://doi.org/10.1016/j.bbabi.2008.02.005>

707 Robertson, P.K.J., Lawton, L.A., Cornish, B.J.P.A., 1999. The Involvement of
708 Phycocyanin Pigment in the Photodecomposition of the Cyanobacterial Toxin,
709 Microcystin-LR. J. Porphyr. Phthalocyanines 3, 544–551.
710 [https://doi.org/10.1002/\(sici\)1099-1409\(199908/10\)3:6/7<544::aid-
711 jpp173>3.0.co;2-7](https://doi.org/10.1002/(sici)1099-1409(199908/10)3:6/7<544::aid-jpp173>3.0.co;2-7)

712 Sinha, A.K., Eggleton, M.A., Lochmann, R.T., 2018. An environmentally friendly
713 approach for mitigating cyanobacterial bloom and their toxins in hypereutrophic
714 ponds: Potentiality of a newly developed granular hydrogen peroxide-based
715 compound. Sci. Total Environ. 637–638, 524–537.
716 <https://doi.org/10.1016/j.scitotenv.2018.05.023>

717 Song, J., Wang, Xuejiang, Ma, J., Wang, Xin, Wang, J., Xia, S., Zhao, J., 2018. Removal
718 of *Microcystis aeruginosa* and Microcystin-LR using a graphitic-C₃N₄/TiO₂ floating
719 photocatalyst under visible light irradiation. Chem. Eng. J. 348, 380–388.
720 <https://doi.org/10.1016/j.cej.2018.04.182>

721 Spoo, L., Catherine, A., 2017. Cyanobacteria samples: preservation, abundance and
722 biovolume measurements, in: Meriluoto, J., Spoo, L., A. Codd, G. (Eds.), Handbook
723 of Cyanobacterial Monitoring and Cyanotoxin Analysis. John Wiley & Sons,
724 Chichester, UK, pp. 526–537. <https://doi.org/10.1002/9781119068761>

725 Stanier, R.Y., Kunisawa, R., Mandel, M., Cohen-Bazire, G., 1971. Purification and
726 properties of unicellular blue-green algae (order *Chroococcales*). Bacteriol. Rev. 35,
727 171–205. <https://doi.org/10.1128/membr.35.2.171-205.1971>

728 Stirbet, A., Lazár, D., Papageorgiou, G.C., Govindjee, 2018. Chlorophyll *a* Fluorescence
729 in Cyanobacteria: Relation to Photosynthesis, Cyanobacteria: From Basic Science
730 to Applications. <https://doi.org/10.1016/B978-0-12-814667-5.00005-2>

- 731 Summerfelt, S.T., 2003. Ozonation and UV irradiation - An introduction and examples of
732 current applications. *Aquac. Eng.* 28, 21–36. [https://doi.org/10.1016/S0144-](https://doi.org/10.1016/S0144-8609(02)00069-9)
733 8609(02)00069-9
- 734 Tao, Y., Hou, D., Zhou, T., Cao, H., Zhang, W., Wang, X., 2018. UV-C suppression on
735 hazardous metabolites in *Microcystis aeruginosa*: Unsynchronized production of
736 microcystins and odorous compounds at population and single-cell level. *J. Hazard.*
737 *Mater.* 359, 281–289. <https://doi.org/10.1016/j.jhazmat.2018.07.052>
- 738 Triantis, T.M., Fotiou, T., Kaloudis, T., Kontos, A.G., Falaras, P., Dionysiou, D.D., Pelaez,
739 M., Hiskia, A., 2012. Photocatalytic degradation and mineralization of microcystin-
740 LR under UV-A, solar and visible light using nanostructured nitrogen doped TiO₂. *J.*
741 *Hazard. Mater.* 211–212, 196–202. <https://doi.org/10.1016/j.jhazmat.2011.11.042>
- 742 Vilela, W.F.D., Minillo, A., Rocha, O., Vieira, E.M., Azevedo, E.B., 2012. Degradation of
743 [D-Leu]-Microcystin-LR by solar heterogeneous photocatalysis (TiO₂). *Sol. Energy*
744 86, 2746–2752. <https://doi.org/10.1016/j.solener.2012.06.012>
- 745 Wang, Xin, Wang, Xuejiang, Zhao, J., Song, J., Su, C., Wang, Z., 2018. Surface modified
746 TiO₂ floating photocatalyst with PDDA for efficient adsorption and photocatalytic
747 inactivation of *Microcystis aeruginosa*. *Water Res.* 131, 320–333.
748 <https://doi.org/10.1016/j.watres.2017.12.062>
- 749 Wang, Xin, Wang, Xuejiang, Zhao, J., Song, J., Wang, J., Ma, R., Ma, J., 2017. Solar
750 light-driven photocatalytic destruction of cyanobacteria by F-Ce-TiO₂/expanded
751 perlite floating composites. *Chem. Eng. J.* 320, 253–263.
752 <https://doi.org/10.1016/j.cej.2017.03.062>
- 753 Wilson, A.E., Wilson, W.A., Hay, M.E., 2006. Intraspecific variation in growth and
754 morphology of the bloom-forming cyanobacterium *Microcystis aeruginosa*. *Appl.*
755 *Environ. Microbiol.* 72, 7386–7389. <https://doi.org/10.1128/AEM.00834-06>
- 756 Yang, W., Tang, Z., Zhou, F., Zhang, W., Song, L., 2013. Toxicity studies of tetracycline
757 on *Microcystis aeruginosa* and *Selenastrum capricornutum*. *Environ. Toxicol.*
758 *Pharmacol.* 35, 320–324. <https://doi.org/10.1016/j.etap.2013.01.006>
- 759 Yang, Z., Kong, F., Shi, X., Yu, Y., Zhang, M., 2015. Effects of UV-B radiation on
760 microcystin production of a toxic strain of *Microcystis aeruginosa* and its
761 competitiveness against a non-toxic strain. *J. Hazard. Mater.* 283, 447–453.
762 <https://doi.org/10.1016/j.jhazmat.2014.09.053>
- 763 Zhao, C., Pelaez, M., Dionysiou, D.D., Pillai, S.C., Byrne, J.A., O’Shea, K.E., 2014. UV
764 and visible light activated TiO₂ photocatalysis of 6-hydroxymethyl uracil, a model

765 compound for the potent cyanotoxin cylindrospermopsin. Catal. Today 224, 70–76.
766 <https://doi.org/10.1016/j.cattod.2013.09.042>

767 Zilliges, Y., Kehr, J.C., Meissner, S., Ishida, K., Mikkat, S., Hagemann, M., Kaplan, A.,
768 Börner, T., Dittmann, E., 2011. The cyanobacterial hepatotoxin microcystin binds to
769 proteins and increases the fitness of *Microcystis* under oxidative stress conditions.
770 PLoS One 6. <https://doi.org/10.1371/journal.pone.0017615>

771